Virology Journal

RESEARCH

Open Access

HSV-1 immune escapes in microglia by down-regulating GM130 to inhibit TLR3-mediated innate immune responses

Jia Liu[1,2†], Xiqian Chen[1,2†], Junxian Liu[1,2], Hainan Zhang[1,2] and Wei Lu[1,2*]

Abstract

Background To investigate the mechanism of Golgi matrix protein 130(GM130) regulating the antiviral immune response of TLR3 after herpes simplex virus type 1(HSV-1) infection of microglia cells. We explored the regulatory effects of berberine on the immune response mediated by GM130 and TLR3.

Methods An in vitro model of HSV-1 infection was established by infecting BV2 cells with HSV-1.

Results Compared to the uninfected group, the Golgi apparatus (GA) fragmentation and GM130 decreased after HSV-1 infection; TLR3 increased at 6 h and began to decrease at 12 h after HSV-1 infection; the secretion of interferon-beta(IFN-β), tumour necrosis factor alpha(TNF-α), and interleukin-6(IL-6) increased after infection. Knockdown of GM130 aggravated fragmentation of the GA and caused TLR3 to further decrease, and the virus titer also increased significantly. GM130 knockdown inhibits the increase in TLR3 and inflammatory factors induced by TLR3 agonists and increases the viral titer. Overexpression of GM130 alleviated fragmentation of the GA induced by HSV-1, partially restored the levels of TLR3, and reduced viral titers. GM130 overexpression reversed the reduction in TLR3 and inflammatory cytokine levels induced by TLR3 inhibitors. Therefore, the decrease in GM130 levels caused by HSV-1 infection leads to increased viral replication by inhibiting TLR3-mediated innate immunity. Berberine can protect the GA and reverse the downregulation of GM130, as well as the downregulation of TLR3 and its downstream factors after HSV-1 infection, reducing the virus titer.

Conclusions In microglia, one mechanism of HSV-1 immune escape is disruption of the GM130/TLR3 pathway. Berberine protects the GA and enhances TLR3-mediated antiviral immune responses.

Keywords Herpes simplex virus type 1 (HSV-1), Toll-like receptor 3, Microglia, Innate immune response, Golgi matrix protein 130

Background

Herpes simplex encephalitis (HSE) is the most common form of encephalitis worldwide. Herpes simplex virus type 1 (HSV-1) causes HSE in > 90% of adult patients with HSE [1]. The global incidence of HSE is 1.57 cases per 100,000 individuals per year. With the use of antiviral drugs, such as acyclovir (ACV), the mortality rate of HSE has decreased to < 20%, but 58% of survivors remain with varying degrees of neurological sequelae, which impose a heavy economic and psychological burden on patients and their families and seriously endanger human

†Jia Liu and Xiqian Chen are contributed equally as co-first authors.

*Correspondence:
Wei Lu
luwei0338@csu.edu.cn
[1] Department of Neurology, Second Xiangya Hospital, Central South University, No. 139, Renmin Middle Road, Changsha, Hunan, China
[2] Clinical Medical Research Center for Stroke Prevention and Treatment of Hunan Province, Department of Neurology, Second Xiangya Hospital, Central South University, No. 139, Renmin Middle Road, Changsha, Hunan, China

health [2, 3]. In addition, recurrence and exacerbation of neurological dysfunction occurred in about 526% of patients [4]. The pathogenesis of HSE has remained unclear for decades, but numerous studies have shown that the innate immune response plays a key role in the early stages of antiviral infection [5, 6].

The innate immune response is the primary line of defense against external pathogens. Toll-like receptors (TLRs) are pattern recognition receptors located in innate immune cells that are key players in early defense against viral infections by activating a range of innate immune signaling pathways [7]. Microglia are resident innate immune cells in the central nervous system (CNS) and are essential to maintain homeostasis in the internal environment of the CNS [8]. Microglia-deficient mice showed reduced secretion of antiviral cytokines and increased viral replication during the early stages of HSV-1 infection [9]. TLR3 is a key protein for microglia to recognize the HSV-1 and produce the antiviral cytokine IFN-α, tumor necrosis factor-α (TNF-α), and interleukin-6 (IL-6) [7, 10–15]. In patients with HSE and mouse models, the lack of TLR3 or its downstream signaling pathway molecules results in defective production of TLR3-dependent antiviral IFNs, leading to increased host susceptibility to HSE [16–18].

Emerging studies have shown that the Golgi apparatus (GA) can serve as an intracellular signaling platform to promote various innate immune pathways, such as TLR and cGAS-STING signaling [19]. Golgi matrix protein 130 (GM130), which is localized in cis-GA, was once thought to be a structural protein; however, it has now been found to have biological functions, such as maintaining the normal structure of GA, regulating protein glycosylation, and maintaining vesicular transport [20]. The normal immune function of TLR3 cannot be separated from the post-translational glycosylation modification of TLR3 by GA [21]. Deglycosylated TLR3 proteins are less stable, easily decomposed, and present at low levels in vivo [22]. Therefore, exploring the effects of changes in GM130 levels on TLR3 after HSV-1 infection in microglia may reveal new therapeutic targets for the treatment of HSE.

Berberine (BBR) is an isoquinoline alkaloid extracted from Berberis vulgaris and other Berberis species. It has pharmacological effects, such as anti-infective, anti-arrhythmic, blood lipid and glucose regulation, and anti-tumor [23–26]. In recent years, studies on the regulation of the immune system by BBR have gradually attracted the interest of scholars [27, 28]. Emerging evidence suggests that BBR regulates inflammatory signaling pathways and their downstream molecules in immune cells [28]. BBR has an inhibitory effect on a variety of viruses, including influenza, hepatitis C, and cytomegalovirus [29]. Based on the immunomodulatory and antiviral functions of BBR, we speculated that BBR could be an effective drug for the treatment of HSE by modulating the TLR3-mediated antiviral immune response or directly inhibiting the activity of HSV-1.

In conclusion, this study explored the relationship between GM130 and TLR3-mediated innate immune responses in microglia after HSV-1 infection and explored whether BBR could modulate innate immune responses to suppress HSV-1.

Methods

Cells and cell cultures

BV2 cells (Procell-CL-0493) derived from C57BL/6 mice have been widely used to study neurological infections and neuroinflammation. Furthermore, HSV-1 was amplified from African green monkey kidney cells in vero cells (ATCC-CRL-1586). Both cells were cultured in high glucose medium (DMEM) (10% premium fetal bovine serum, 1% double antibody) in a humid incubator with 5% CO_2 at 37 °C.

Microglia infection and reagents

The HSV-1 strain used in this study was obtained from the School of Life Sciences of Central South University. BV2 cells were infected with HSV-1 with a multiplicity of infection (MOI) of 1. Furthermore, BV2 cells were treated with the TLR3 agonist (Poly (I:C) [10 μg/ml]) and TLR3 inhibitor (TLR3i [10 μM]) 6 h before sample collection to activate/inhibit the expression of TLR3. To observe the effects of BBR hydrochloride (Sigma, Cat#BP1108) and BBR in combination with ACV (MCE, Cat#HY-17422), we used BBR (0, 3, 10 uM), ACV (3 μM), and BBR (3 uM) + ACV (3 uM) treating BV2 cells separately at 24 h before sample collection.

Cell counting kit-8 (CCK-8) assay

Cells were treated according to the manufacturer's instructions (NCM Biotech, cat# C6005) and cell viability was assessed 24 h after treatment using the CCK-8 assay. The optical density was recorded at 450 nm.

Determination of HSV-1 growth curve

BV2 cells were inoculated in 6-well plates at a density of 5×105 cells/ml, and HSV-1 stock solution was mixed with culture medium in each well by MOI = 1 (one-step growth curve), and then the mixture was incubated in an incubator at 37 °C. At 0, 6, 12, 24, and 48 h of incubation, the culture medium was centrifuged and the supernatant was collected to detect the titers of HSV-1 by virus plaque assay.

Virus titer determination

The titers of HSV-1 were measured using an empty plaque formation test. When the density of vero cells was approximately 70% in the 24-well plate, the gradient diluent of HSV-1 solution (10–1, 10–2, 10–3, 10–4, 10–5, 10–6, 10–7) was added to the plate several times to the well and then placed in an incubator at 37 °C for 3 h. The culture medium in the wells was mixed with 2% sterilized agarose and cooled to room temperature until solidification. After that, the 24-well plate was incubated at 37 °C in an incubator with 5% CO2 for 2 d of culture. After incubation, a plaque count was performed and the average value of three parallel tests was recorded.

RNAi-mediated GM130 silencing

BV2 cells were transfected with small interfering RNA GM130/control (siGM130/siCtrl) at a density close to 70%. We used PepMute (SignaGen) as a vector to transfect SiCtrl and siGM130 (both purchased from Gene Pharma in Suzhou and verified in our previous studies) into BV2 cells. Cell samples were collected for detection 48 h post-transfection.

Plasmid-mediated overexpression of GM130

BV2 cells were transfected with the GM130 pcDNA3.1 (+) plasmid (Sangon Biotech, Shanghai, China) at a density of 6070%. The GM130 plasmid was transfected into BV2 cells using lipofectamine 3000 as a vector (Invitrogen; Cat# L3000150). Cell samples were collected for detection 48 h post-transfection.

Immunoblotting

Cells were lysed using a radioimmunoprecipitation assay containing 1% protease and 1% phosphatase inhibitors. Proteins were separated by SDS-PAGE and transferred to a polyvinylidene fluoride (PVDF) membrane (microporous, Cat# ISEQ00010). The following primary antibodies and secondary antibodies were used for immunoblotting. Primary antibodies include GM130 antibody (BD Bioscience, Cat# 610822), TLR3 antibody (Abcam, Cat# ab62566), P115 antibody (Ptoteintech, Cat# 13509-1-AP), HSV-1 antibody (Santa cruz, Cat# sc-57863), β-actin (Proteintech, Cat# 10494-1-AP). Secondary antibodies include horseradish peroxidase-labeled goat anti-mouse IgG (Proteintech, Cat# 15014) and horseradish peroxidase-labeled goat Anti-Rabbit IgG (Abiowell, Cat# AWS0002b). Liquids A and B of the chemiluminescent reagent were mixed evenly in equal volumes and the mixture was added to the PVDF membrane and incubated for approximately 30 s in the dark. The PVDF membrane was then placed on a chemiluminescent imager for imaging.

Immunofluorescence staining

BV2 cells were fixed on slides with 4% paraformaldehyde (PFA) in the dark. Next, 0.3% TritonX-100 was used to penetrate the membrane of BV2 cells. At room temperature, the sample was blocked with a 5% BSA blocking solution for 1 h. The P115 antibody (Proteintech, Cat# 13509-1-AP), GM130 antibody (Boster, Cat# M05865-2), and IBA1 antibody (Servicebi, Cat# GB11105) were used to incubate the sample overnight at 4 °C. Cy3-labeled goat anti-rabbit IgG (Servicebio, Cat# GB21303) and FITC-labeled goat anti-mouse IgG (Servicebio, Cat# GB22301) were used to incubate the sample for 1 h at 25 °C in the dark. The nuclei were then stained with DAPI (Sigma, Cat# D9542). A confocal fluorescence microscope (OLYMBUS) was used for imaging.

Enzyme-linked immunosorbent assay (ELISA)

The supernatant of the BV2 cell culture was centrifuged at 1000×*g*, 4 °C for 15 min. The levels of IFN-β, TNF-α, and IL-6 were measured in the supernatant. The experimental procedures were performed according to the instructions of the ELISA kit for IFN-β (CUSABIO, cat# CSB-E04945m), TNF-α (CUSABIO, cat# CSB-E04744m), and IL-6 (CUSABIO, cat# CSB-E04639m).

Transmission electron microscopy

Cells were fixed overnight at 4 °C with 2.5% glutaraldehyde. Samples were rinsed with 0.1 M phosphoric acid buffer (Na2HPO4, pH = 7), fixed with 1% osmic acid at room temperature, and then rinsed with phosphoric acid buffer. The samples were sequentially dehydrated with 30%, 50%, 70%, 80%, 85%, 90%, 95%, and 100% ethanol for 15 min. The samples were then treated with pure acetone for 20 min and impregnated with epoxy resin for 48 h. Cells were restained with 2% uranium dioxyacetate and 0.2% lead citrate for 15 min at room temperature, then samples were dried overnight. we measured the Golgi cisternae lumen width (μm) in these samples. We quantified the maximum length of GA cisternae (designated as maximum luminal width) by measuring the cisternae diameters assuming circular structures. Twenty cells for each condition and 3 GA cisternae for each cell were analyzed by transmission electron microscopy. Each image was measured with ImageJ software.

The ultrastructure of the cells in the samples was observed by transmission electron microscope (Tecnai G2 20 TWIN FEI).

Statistical analysis

The experimental data were statistically analyzed using GraphPad Prism 8.4.0 (GraphPad Software, San Diego, California, USA). All data were obtained from at least three independent experiments. Experimental data are expressed as X ± SD. The significance of the experimental data for the two samples was analyzed using a two-sample t-test. When $p > 0.05$, there were no significant differences between the two groups (ns). When $p < 0.05$, a statistically significant difference was observed between the two groups (*, #, $). $p < 0.01$ was considered a statistically significant difference between the two groups (**, ##, $$). $p < 0.001$ was considered an extremely significant statistical difference between the two groups (***, ###, $$$).

Results

After HSV-1 infection, GM130 and TLR3 were downregulated and the GA was fragmented

We observed the cell morphology of BV2 cells infected with HSV-1 at different time points using light microscopy. The results showed that as the infection progressed, the protrusions of the cells increased, as well as the proportion of cells with spindle morphology and amoebia-like morphology. There were multiple vacuoles in the cytoplasm of the cells, cell spacing increased, and some cells were detached and suspended (Fig. 1a), with an increased multipolar percentage (mock, 6% vs. 6 h, 8% vs. 12 h, 29% vs. 24 h, 35%). A one-step growth curve was used to determine the characteristics of HSV-1 proliferation in BV2 cells. The results suggested that the titer of HSV-1 reached a plateau at 36–48 h after infection, with a maximum titer of 9.0×10^5 PFU/ml (Fig. 1b), followed by a gradual decrease in viral load. HSV-1 envelope glycoprotein gD (HSV-gD) gradually increased with increasing infection time, indicating that HSV-1 infected microglia and expanded. It began 12 h after HSV-1 infection, and GM130 protein levels gradually decreased ($p < 0.001$, Fig. 1c–f). The TLR3 protein increased after 6 h of HSV-1 infection ($p < 0.001$) but decreased significantly after 12 and 24 h of HSV-1 infection ($p < 0.001$) (Fig. 1d, g).

After 6 and 12 h of HSV-1 infection, IFN-β, TNF-α, and IL-6 secreted by BV2 cells increased significantly ($p < 0.001$). In BV2 cells, IFN-β, TNF-α, and IL-6 decreased significantly 24 h after HSV-1 infection compared to 12 h after HSV-1 infection ($p < 0.05$, $p < 0.01$, and $p < 0.05$, respectively) (Fig. 1h). The destruction of the GA is becoming increasingly serious. In uninfected cells, immunofluorescence showed tightly packed GA structures in the perinuclear area (labeled with GM130 and P115), while this structure and the intracellular localization of GA were not destroyed after 6 h of HSV-1 infection. At 12 h after HSV-1 infection, GA was fragmented and dispersed in the cytoplasm. At 24 h after infection, the structural damage to GA was more severe and the fluorescence intensity of GM130 decreased significantly (Fig. 2a, b, Supplementary Fig. 1).

Our findings suggested that with the prolongation of HSV-1 infection, the Golgi apparatus was destroyed in microglia, and the expression of GM130, TLR3 and inflammatory factors is reduced.

Knockdown of GM130 can inhibit the level of TLR3 and lead to structural damage to the GA

BV2 cells were transfected with siRNA for 36 h and then infected with HSV-1 (MOI = 1) for 12 h. The results showed that GM130 was successfully knocked down in the uninfected group and the HSV-1 infected group ($p < 0.001$ and $p < 0.001$, respectively), while the TLR3 protein was significantly decreased ($p < 0.001$ and $p < 0.001$, respectively) (Fig. 3a, b, d, e). Furthermore, compared to the HSV-1 + SiCtrl group, the expression of HSV-1 protein increased significantly in the HSV-1 + SiGM130 group ($p < 0.001$, Fig. 3b, e), and the titers of HSV-1 were significantly higher in the HSV-1 + SiGM130 group than in the HSV-1 + SiCtrl group ($p < 0.01$) (Fig. 3c). These results showed that GM130 regulates the level of TLR3 and affects the replication of HSV-1 in BV2 cells.

(See figure on next page.)

Fig. 1 After HSV-1 infection, change in microglial morphology and GM130, TLR3, and inflammatory cytokines. **a** Cell morphology and statistical results of BV2 cells at 6, 12, and 24 h after Mock and HSV-1 infection. HSV-1-infected BV2 cells with MOI = 1 and observed cell morphology under an inverted microscope (amoeba morphology is shown by a black arrow). The cell morphology statistics at each time point are obtained from three different visual fields, with a scale of 50 μm. **b** One-step growth curve of HSV-1 in BV2 cells. HSV-1 infection infects BV2 cells with MOI = 1. **c**, **d** Protein levels of GM130, TLR3, and HSV-1 are analyzed semiquantitatively by scanning a grayscale, and βactin is used as internal parameter correction. The expression levels of GM130, TLR3, and HSV-1 are homogenized at each time point compared to those of the uninfected group. Semiquantitative results of **e** are shown in **f** and **g**. **h** The secretion levels of the inflammatory cytokines IFN-β, TNF-α, and IL-6 in the medium are detected by ELISA. Data are obtained through three independent replicates, expressed as X ± SD, and statistically analyzed between the two groups using a t-test. ns, *, **, *** represent other groups vs. Mock group; ns, #, ##, ##, and ## represent the comparison between the two groups marked with a short horizontal line. ns, $p > 0.05$; *, #, $p < 0.05$; **, ##, $p < 0.01$; ***, ###, $p < 0.001$

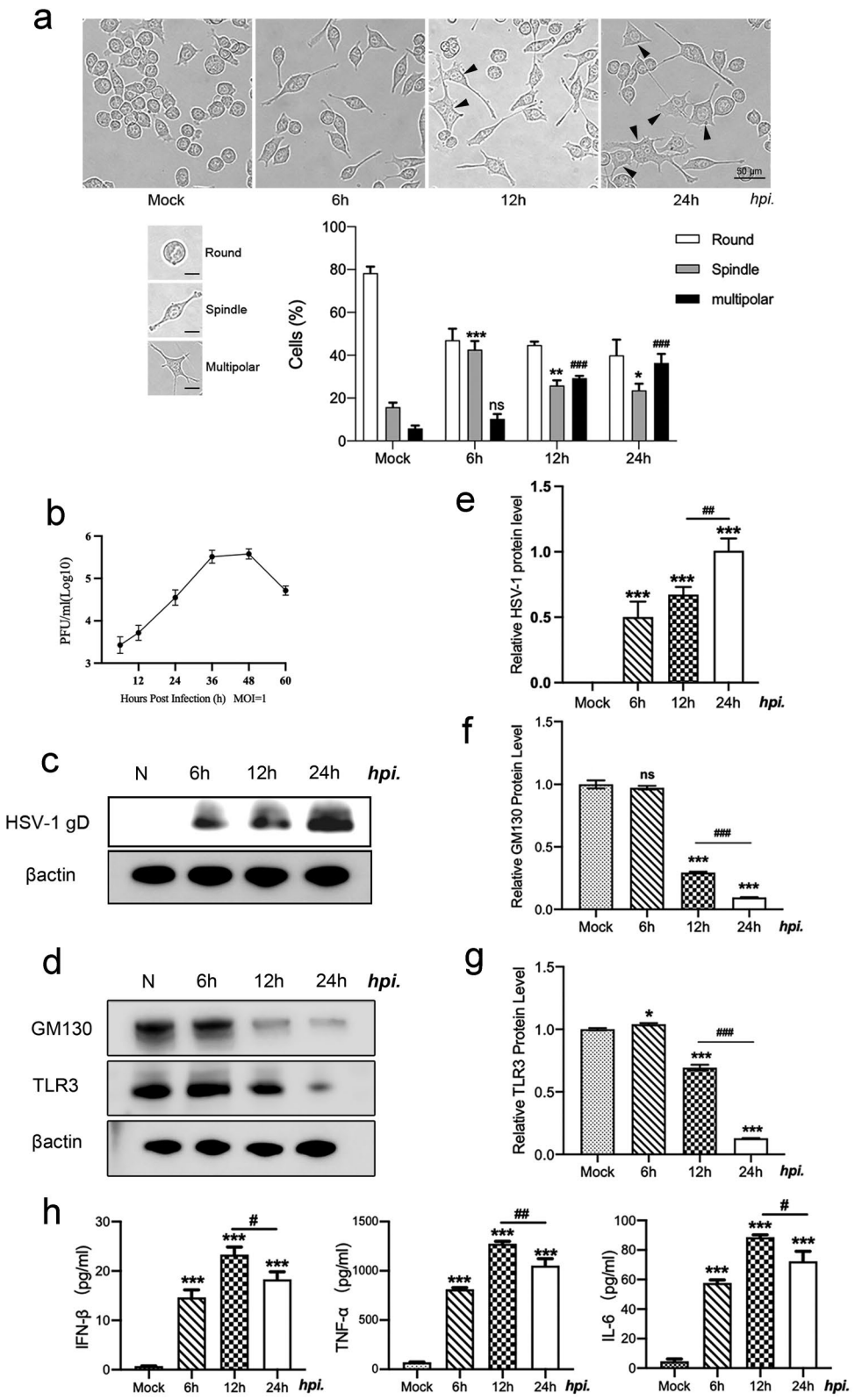

Fig. 1 (See legend on previous page.)

The immunofluorescence results showed that the knockdown of GM130 and infection with HSV-1 caused structural fragmentation of GA in BV2 cells, and the fragmented GA was dispersed in the cytoplasm. After 12 h of HSV-1 infection of BV2 cells, GM130 knockdown caused further structural damage to GA (Fig. 4a, b). These results were also confirmed when we used transmission electron microscopy to observe the structural damage to the GA. Compared to the tight and ordered GA structure in the uninfected group, the GA became swollen and disordered in the group infected with HSV-1. Swelling and disordered GA were also observed when GM130 was knocked down without HSV-1 infection (Fig. 4c, supplementary Fig. 2).Quantitation of the maximum luminal width of the Golgi cisternae (μm) revealed a significant damage of GA structure ($p < 0.001$, Fig. 4d).

Overexpression of GM130 can upregulate the level of TLR3 and reverse the damage to the GA

BV2 cells were transfected with the pcDNA3.1 GM130 plasmid for 36 h and then infected with HSV-1 (MOI = 1) for 12 h or not. The results showed that GM130 was significantly overexpressed in the uninfected and 12 h post-infection groups ($p < 0.001$ and $p < 0.001$, respectively). Under uninfected conditions, GM130 overexpression did not affect the level of TLR3 ($p > 0.05$). However, 12 h after HSV-1 infection, GM130 overexpression significantly increased the level of TLR3 ($p < 0.001$) (Fig. 5a, b, d, e). Compared to the HSV-1 + SiCtrl group, the expression of the HSV-1 protein decreased significantly in the HSV-1 + OEGM130 group ($p < 0.001$, Fig. 5b, e). Compared to the HSV-1 + SiCtrl group, the titer of HSV-1 decreased significantly in the HSV-1 + OEGM130 group ($p < 0.05$) (Fig. 5c). These results suggest that GM130 upregulates TLR3 and inhibits HSV-1 replication in BV2 cells infected with HSV-1.

In addition, structural changes in GA after GM130 overexpression were detected by immunofluorescence and transmission electron microscopy. GM130 overexpression protected the GA structure from fragmentation and partially restored its tight structure around the nucleus (Fig. 6a, b). Overexpression of GM130 reversed the swelling and fragmentation of GA caused by HSV-1 infection and remodeled the structure of GA by transmission electron microscopy (Fig. 6c, supplementary Fig. 3). Further Quantitation of the maximum luminal width of the Golgi cisternae (μm) confirmed the above findings (Fig. 6d). Therefore, we found that GM130 regulates the expression of TLR3 and influences viral proliferation.

TLR3 agonists reverse the knockdown of GM130-induced downregulation of TLR3 and inflammatory factors

In HSV-1-infected BV2 cells, to verify whether GM130 affects the secretion of inflammatory cytokines by regulating TLR3, we knocked down GM130 in BV2 cells and then treated them with a TLR3 agonist [Poly (I:C), PIC].

Compared to the HSV-1 group, the level of TLR3 increased significantly in the HSV-1 + Poly (I:C) group ($p < 0.001$) (Fig. 7a, c); meanwhile, the secretion of the inflammatory cytokines IFN-β, TNF-α, and IL-6 increased significantly in the HSV-1 + Poly (I:C) group than in the HSV-1 group ($p < 0.001$, $p < 0.001$, and $p < 0.001$, respectively) (Fig. 7d–f). Compared to the HSV-1 group, the expression of HSV-1 protein decreased significantly in the HSV-1 + Poly (I:C) group ($p < 0.05$, Fig. 7a, d); however, the level of GM130 was not significantly different between the two groups ($p > 0.05$) (Fig. 7a, b). Compared to the HSV-1 + SiGM130 group, the level of TLR3, IFN-β, TNF-α, and IL-6 increased significantly in the HSV-1 + SiGM130 + Poly (I:C) group ($p < 0.001$, $p < 0.001$, $p < 0.001$, and $p < 0.001$, respectively) (Fig. 7a, c, e), while the expression of HSV-1 protein was decreased in the HSV-1 + SiGM130 + Poly (I:C) group ($p < 0.01$, Fig. 7a, d). These results suggest that the downregulation of GM130 can reduce inflammatory factors associated with microglia by inhibiting TLR3, thus increasing HSV-1 activity.

TLR3 inhibitors can reverse the upregulation of TLR3 and inflammatory cytokines caused by the overexpression of GM130

After GM130 overexpression, BV2 cells were treated with a TLR3 inhibitor (TLR3i). The level of TLR3 was

(See figure on next page.)

Fig. 2 Morphological changes of the Golgi apparatus (GA) at different time points after microglia infection with HSV-1. **a** Fluorescence intensity and GA structure of GM130 are observed by immunofluorescence, and IBA1 is used to label microglia cells. Re-stained the nucleus with DAPI (blue channel). Merge the above channels into the same field of view to produce a merged image. Scale, 10 μm. **b** Since the expression of P115 remained unchanged after infection with HSV-1 in BV2 cells, further fluorescence labeling of P115 is performed to observe the structural changes of GA. Re-stained the nucleus with DAPI (blue channel). Scale, 10 μm. In the infected group at different time points, the fluorescently labeled GA structure gradually became loose, from tightly stacked perinuclear to loosely distributed in the cytoplasm (white arrow). The representative images are obtained from three independently repeated experiments. Scale, 10 μm

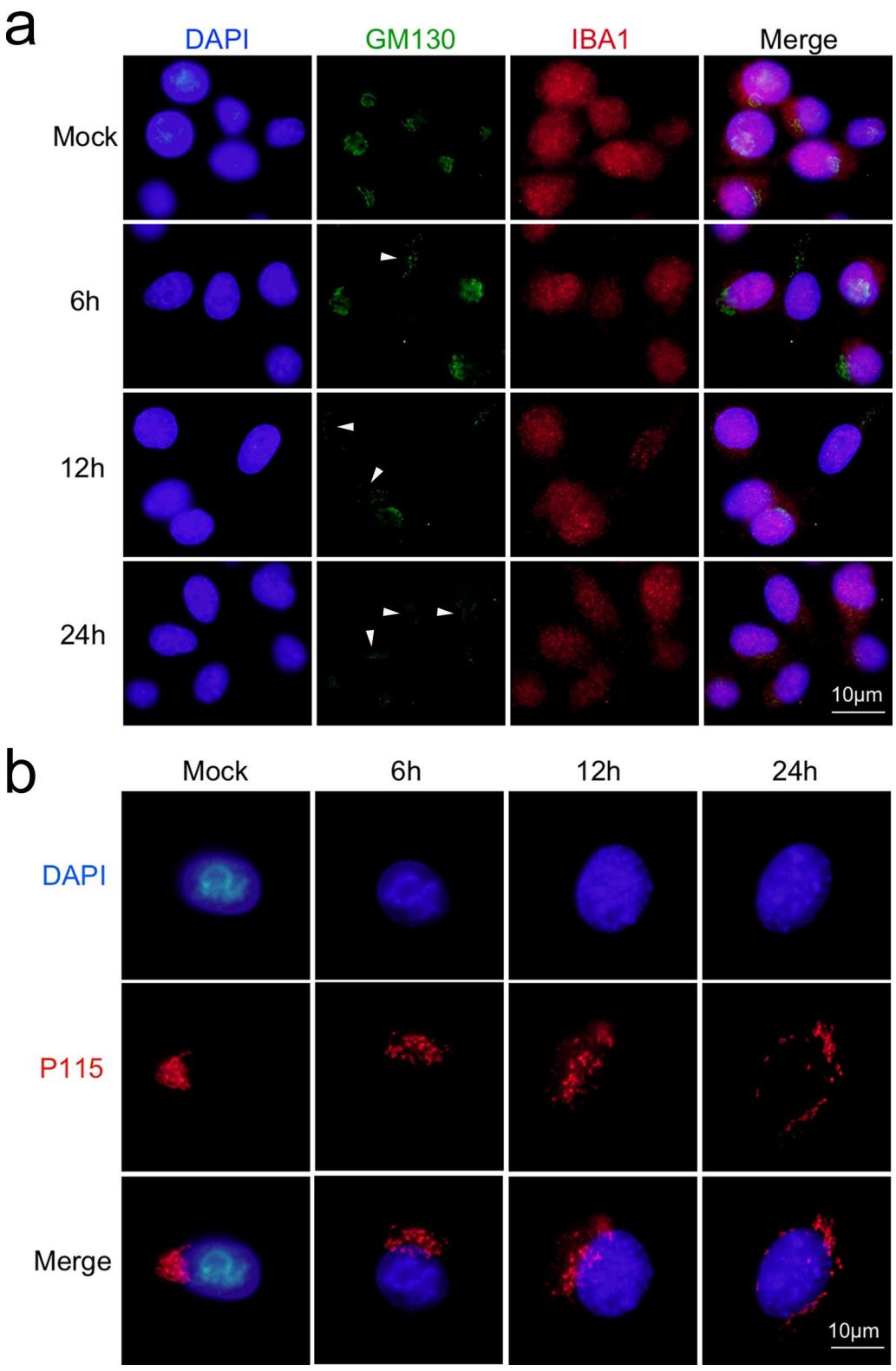

Fig. 2 (See legend on previous page.)

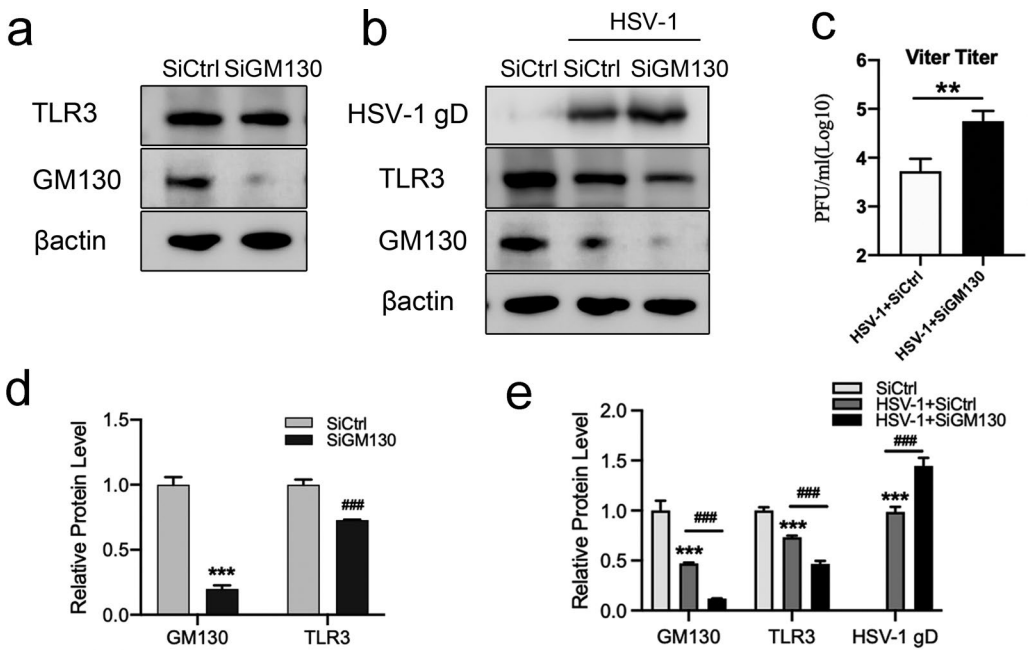

Fig. 3 Changes in knockdown GM130 in uninfected and HSV-1-infected BV2 cells. **a**, **d** Knockdown GM130 without infection and semiquantitative results of knockdown GM130 without infection. **b**, **e** Knockdown GM130 12 h after infection and semi-quantitative results of knockdown GM130 12 h after infection. **c** Effect of siRNA knockdown GM130 on viral replication. Data are obtained through three independent replicates, expressed as X ± SD, and statistically analyzed between the two groups using a t-test. *, **, and *** represent the comparison with the NC group. ns, $p > 0.05$; *, #, $p < 0.05$; **, ##, $p < 0.01$; ***, ###, $p < 0.001$

significantly lower in the HSV-1 + TLR3i group than in the HSV-1 group ($p < 0.001$) (Fig. 8a, c). Meanwhile, compared to the HSV-1 group, the secretion of IFN-β, TNF-α, and IL-6 decreased in the HSV-1 + TLR3i group ($p < 0.001$, $p < 0.001$, and $p < 0.001$, respectively) (Fig. 8e). Compared to the HSV-1 group, the expression of HSV-1 protein increased significantly in the HSV-1 + TLR3i group ($p < 0.05$, Fig. 8a, e). There were no significant differences in GM130 levels between the above two groups ($p > 0.05$, Fig. 8a, b). Compared to the HSV-1 + OEGM130 group, the level of TLR3, IFN-β, TNF-α, and IL-6 in the HSV-1 + OEGM130 + TLR3i group was downregulated ($p < 0.05$, $p < 0.001$, $p < 0.001$, and $p < 0.001$, respectively) (Fig. 8a, c, e), while the expression of the HSV-1 protein increased in the HSV-1 + OEGM130 + TLR3i group ($p < 0.05$, Fig. 8a, d)). These results suggest that overexpression of GM130 can promote the secretion of microglia-associated inflammatory cytokines by upregulating TLR3 levels during HSV-1 infection, thus inhibiting HSV-1 activity.

Therefore, GM130 affects the expression of innate immune molecules by regulating TLR3 in microglia. HSV-1 immune escapes in microglia by down-regulating GM130 to inhibit TLR3-mediated innate immune responses.

BBR can reverse Golgi damage and reverse the downregulation of TLR3 and inflammatory cytokines after HSV-1 infection

At 12 h before HSV-1-infected BV2 cells, we treated BV2 cells with BBR at concentrations of 1, 3, and 10 uM. Cell viability was significantly reduced at concentrations up to 10 uM (Fig. 9a). Therefore, we chose 3 uM as the concentration for treatment. BV2 cells were treated with BBR (3 uM) and ACV (3 uM, common concentrations in the reference literature) 12 h before HSV-1 inflected BV2 cells. Compared to the HSV-1 group, the levels of GM130 and TLR3 increased in the HSV-1 + BBR group ($p < 0.01$ and $p < 0.01$, respectively) (Fig. 9b–d), as well as the IFN-β, TNF-α, and IL-6 ($p < 0.01$, $p < 0.01$, and $p < 0.01$, respectively) (Fig. 9f–h). The expression of HSV-1 protein decreased significantly under the treatment of BBR ($p < 0.01$) (Fig. 9b, e), and the titers of HSV-1 also decreased significantly under the treatment of BBR ($p < 0.05$) (Fig. 9i). Compared to the HSV-1 group, the levels of GM130, TLR3, IFN-β, TNF-α, and IL-6 in the HSV-1 + ACV group increased significantly ($p < 0.01$, $p < 0.01$, $p < 0.001$, $p < 0.001$, and $p < 0.001$, respectively) (Fig. 9b–h). The expression of HSV-1 protein decreased significantly with ACV treatment ($p < 0.001$) (Fig. 9b, e), and the titers of HSV-1 also decreased significantly

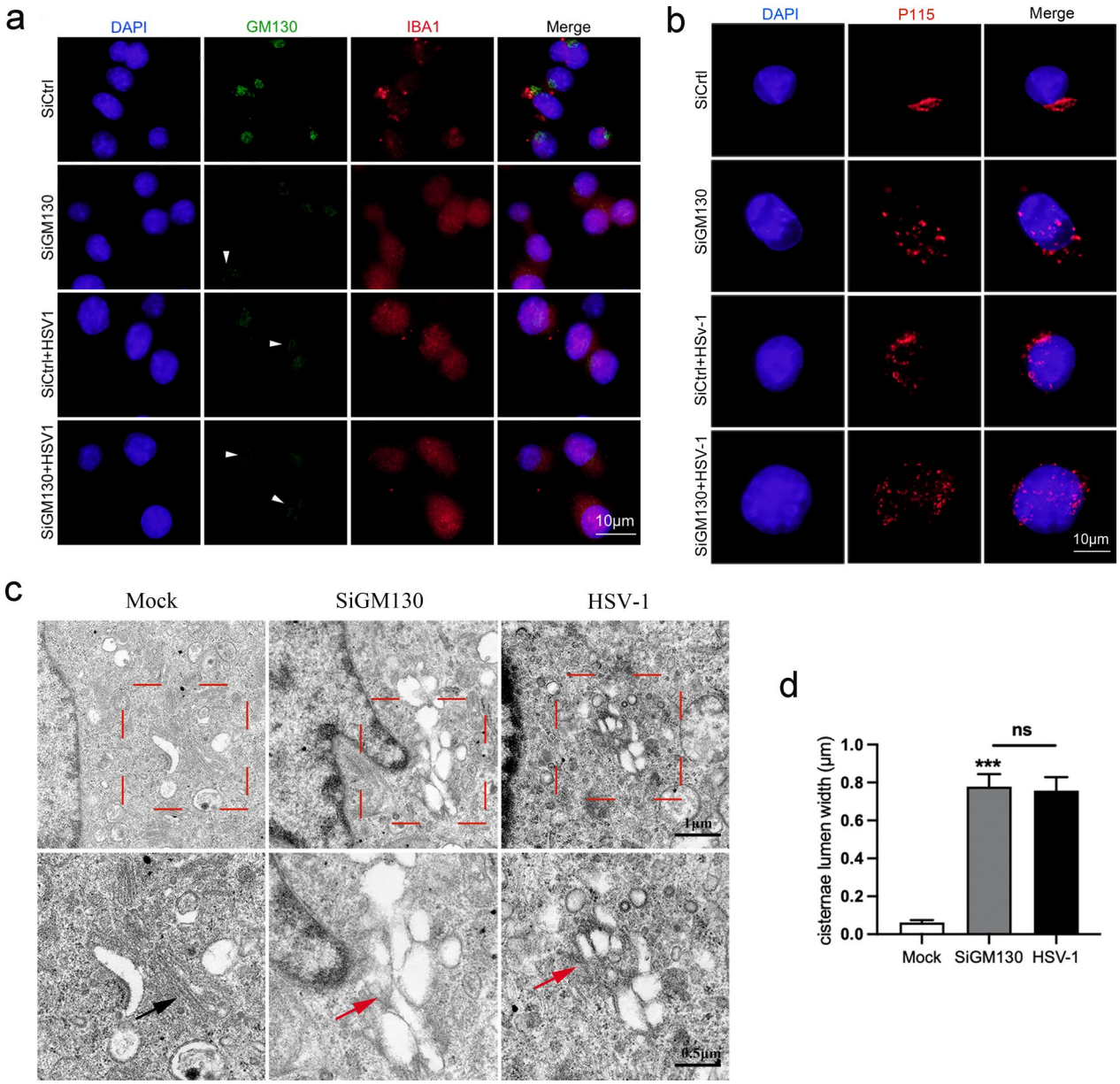

Fig. 4 Structural changes in the Golgi apparatus (GA) after GM130 knockdown in microglia cells. **a** After GM130 knockdown in the uninfected and 12 h infected groups, the GA structure (GM130 marker) is observed by immunofluorescence, and IBA1 is used to label microglia cells. The GA fragmentation is shown in IF (white arrow). Immunostaining is performed for GM130 (green channel) and IBA1 (red channel) of transfected cells, and DAPI (blue channel) re-stained the nucleus. Scale, 10 μm. **b** The GA structure is observed by immunostaining for P115 (red channel) of transfected cells and DAPI (blue channel) re-stained nucleus. Scale, 10 μm. **c** Transmission electron microscopy images of the 12 h infection and GM130 knockdown groups showed GA disruption and swelling of the vesicle structure, from tightly packed (black arrow) to disordered swelling (red arrow). Quantification of Golgi cisternae lumen (μm) in mock- and HSV-1-infected cells and cells transfected with SiGM130. Data represent the average maximum luminal width of the Golgi cisternae from three independent experiments. Data are shown as mean ± SD and were analyzed using the Student's t-test. Representative electron micrographs of the Golgi cisternae in mock- and HSV-1-infected cells and cells transfected with SiGM130. Representative images are obtained from three independent repeated experiments with scales of 1 μm and 0.5 μm

with ACV treatment ($p < 0.001$) (Fig. 9i). These results indicated that both ACV and BBR can up-regulate the GM130/TLR3 pathway and inhibit the virus propagation.

Compared to the HSV-1 + BBR group, the levels of GM130, TLR3, IFN-β, TNF-α, and IL-6 increased significantly in the HSV-1 + BBR + ACV group ($p < 0.01$, $p < 0.01$, $p < 0.01$, $p < 0.01$, and $p < 0.01$, respectively)

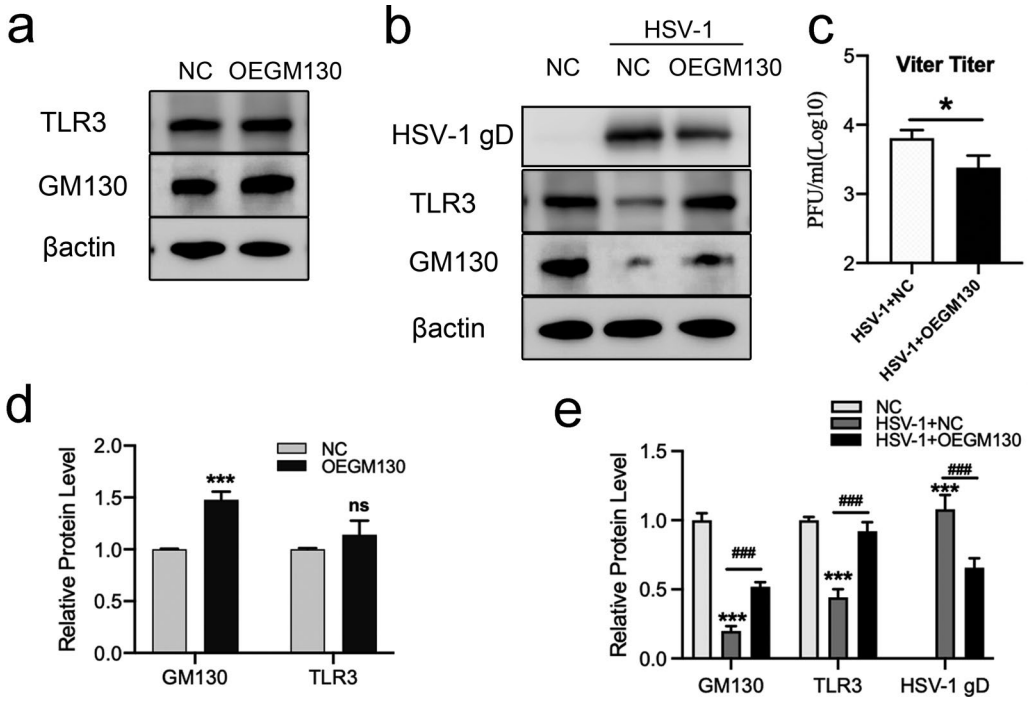

Fig. 5 Changes in overexpression of GM130 in uninfected and HSV-1-infected BV2 cells. **a**, **d** Overexpress GM130 without infection and semiquantitative results of knockdown GM130 without infection. **b**, **e** Overexpress GM130 12 h after infection and semiquantitative results of overexpress GM130 12 h after infection. **c** Effect of Plasmid overexpress GM130 on viral replication. Data were obtained through three independent replicates, expressed as X ± SD, and statistically analyzed between the two groups using a t-test. *, **, *** represent the comparison with the NC group. ns, $p > 0.05$; *, #, $p < 0.05$; **, ##, $p < 0.01$; ***, ###, $p < 0.001$

(Fig. 9b–h), while the expression of HSV-1 protein was decreased in the HSV-1 + BBR + ACV group ($p < 0.05$) (Fig. 9b, e), and the titers of HSV-1 decreased significantly ($p < 0.01$) (Fig. 9i). Compared to the HSV-1 + ACV group, GM130, TLR3, IFN-β, TNF-α, and IL-6 levels increased significantly in the HSV-1 + BBR + ACV group ($p < 0.05$, $p < 0.01$, $p < 0.05$, c5, $p < 0.05$, respectively) (Fig. 9b–h), while the expression of HSV-1 protein had a decreasing trend in the HSV-1 + BBR + ACV group (Fig. 9b, e), and the titers of HSV-1 had a decreasing trend, but did not reach statistical significance (Fig. 9i). Immunofluorescence showed that the structural destruction of GA was reversed (the GA structure was tighter and more ordered), and the fluorescence intensity of GM130 was enhanced in the HSV-1 + BBR group compared to that in the HSV-1 group (Fig. 10). Compared to the HSV-1 infected group, the structure of the GA was also protected (the GA was tighter and more ordered), and the fluorescence intensity of GM130 was stronger in the HSV-1 + ACV group (Fig. 10). The GA was more structurally complete and organized in the HSV-1 + BBR + ACV group compared to that of the HSV-1 + BBR group. Compared to the HSV-1 + ACV group, GA was more structurally complete and organized in the HSV-1 + BBR + ACV group (Fig. 10).

Therefore, the combination of ACV and BBR in anti-HSV-1 therapy is more effective in maintaining the Golgi structure and function and inhibiting viral immune escape than the use of either drug alone.

Discussion

Herpes simplex encephalitis is a fatal infection that affects the central nervous system. Meanwhile, HSV-1 infection can also cause autoimmune encephalitis, Alzheimer's disease, and Parkinson's disease. [30, 31]. In addition to conventional antiviral therapies, immunomodulatory therapies have been the focus of preclinical research. The host's innate immune response, specifically TLR3 signaling, is particularly important for recognizing and clearing HSV-1, inhibiting HSV-1 replication, and activating adaptive immune responses. Recent research has revealed that the GA may be a signal transduction organelle that promotes a variety of innate immune pathways, including the TLR3 signaling pathway [19]. Our previous studies have suggested that HSV-1 can cause downregulation of GM130 and fragmentation of GA, while knocking down GM130 without infection can also induce fragmentation of GA [32]. Furthermore, GM130 is an important regulator of protein glycosylation and TLR3 glycosylation is essential for normal immune

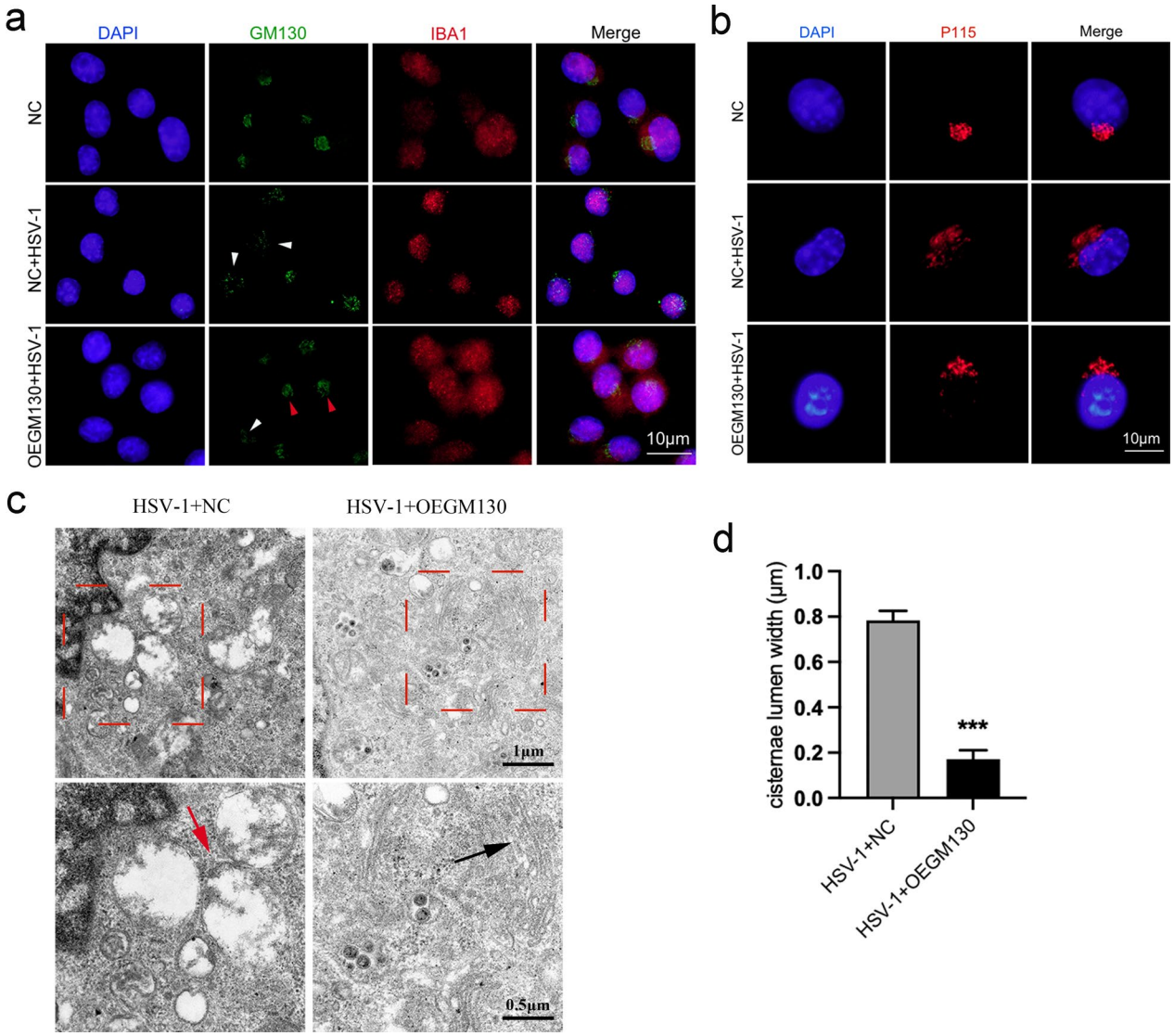

Fig. 6 Structural changes in the Golgi apparatus (GA) after GM130 overexpression in microglia cells. **a** 12 h was selected as the infection time point; 36 h after plasmid transfection, HSV-1 infected cells with MOI = 1, and 12 h after infection, GA structure (GM130 marker) is observed. Scale, 10 μm. **b** HSV-1 infected cells with MOI = 1 at 36 h after plasmid transfection, and GA structure (P115 label) is observed by immunofluorescence at 12 h after infection. Scale, 10 μm. The GM130 and P115 labeled GA structures gradually loosen 12 h after infection, from tightly stacked perinuclear to loosely distributed in the cytoplasm (white arrow). Fluorescently labeled GA structures after overexpression of GM130 partially regain a compact perinuclear distribution (red arrow). The representative images are obtained from three independently repeated experiments. Scale, 10 μm. **c** Transmission electron microscope images after overexpression of GM130 showed that GA improved the swelling and disintegration of GA caused by HSV-1 infection (red arrow) and reshaped the structure of GA (black arrow). **d** Quantification of Golgi cisternae lumen (μm) in group HSV-1 + NC and group HSV-1 + OEGM130. The representative images are obtained from three independently repeated experiments. Scale 1 μm, 0.5 μm

function. Therefore, our study aimed to explore whether GM130 is involved in regulating TLR3, which mediates the innate immune response after HSV-1 infection.

Microglia, one of the most important immune cells in the CNS, mediate immune responses mainly through multiple immune receptors on the cell membrane [33]. TLR3, an important immune receptor in microglia, is involved in recognizing HSV-1 and activating IFN-I production, thus exerting antiviral effects [7]. IFN-1 secreted by microglia, such as IFN-β, plays a key role in limiting the spread of the virus after HSV-1 infection [34, 35]. Furthermore, the TLR3 signaling pathway mediates the secretion of TNF-α and IL-6, which also play a crucial role in the inhibition of HSV-1 [13–15]. HSV-1 may directly or indirectly interfere with the TLR3 signaling pathway in several ways to evade the host's immune

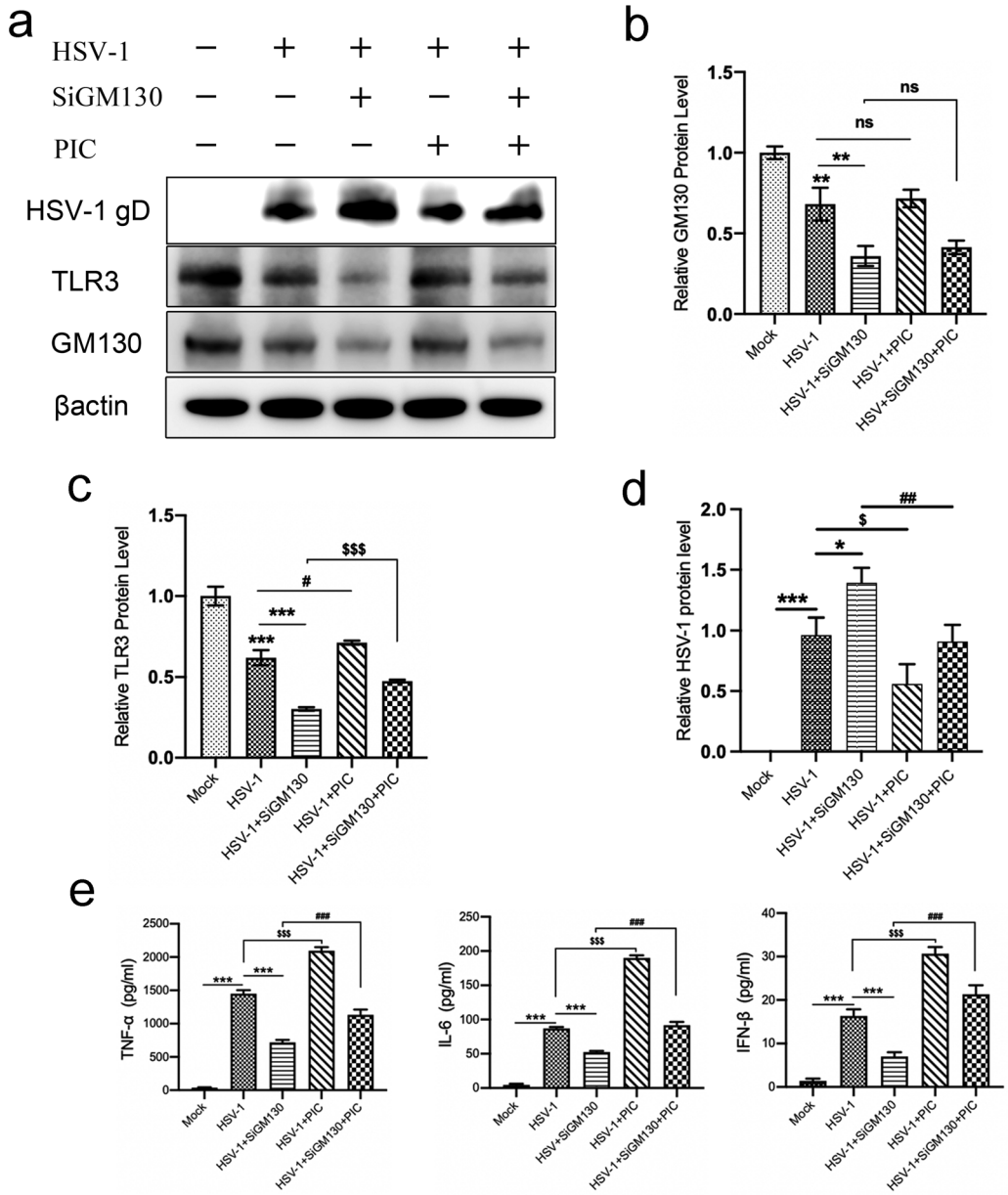

Fig. 7 Effects of Poly (I:C) treatment of GM130 knockdown BV2 cells on TLR3 and inflammatory cytokines. **a** Protein levels of GM130, TLR3, and HSV-1 are treated with Poly (I:C), and βactin is used as the internal parameter correction. Protein levels in each group are homogenized compared to those of the uninfected group. **b** Semi-quantitative results of GM130. **c** Semi-quantitative results of TLR3. **d** Semi-quantitative results of HSV-1 gD. **e** Secretion levels of inflammatory cytokines IFN-β, TNF-α, and IL-6 after Poly (I:C) treatment. Data are obtained through three independent replicates, expressed as X ± SD, and statistically analyzed between the two groups using a t-test. A comparison between the two groups is marked with a dashed line. ns, $p > 0.05$; *, #, $p < 0.05$; **, ##, $p < 0.01$; ***, ###, $p < 0.001$

system [36]. The secretion of these inflammatory cytokines is not exclusively regulated by TLR3 due to the presence of RLRs, CGAS-STING, and NLRs signaling pathways in microglia in response to HSV-1 infection [36]. Therefore, we speculate that this may be the reason the decrease in the secretion of the inflammatory cytokines lagged behind the downregulation of TLR3.

GA stress alters GA gene expression to regulate the GA structure and function in response to external stimuli. Once external stimulation exceeds the upper limit of GA stress, irreversible damage to the GA occurs [37, 38]. He et al. found that GA stress occurred in brain microvascular endothelial cells in response to infection with HSV-1, manifested as downregulation

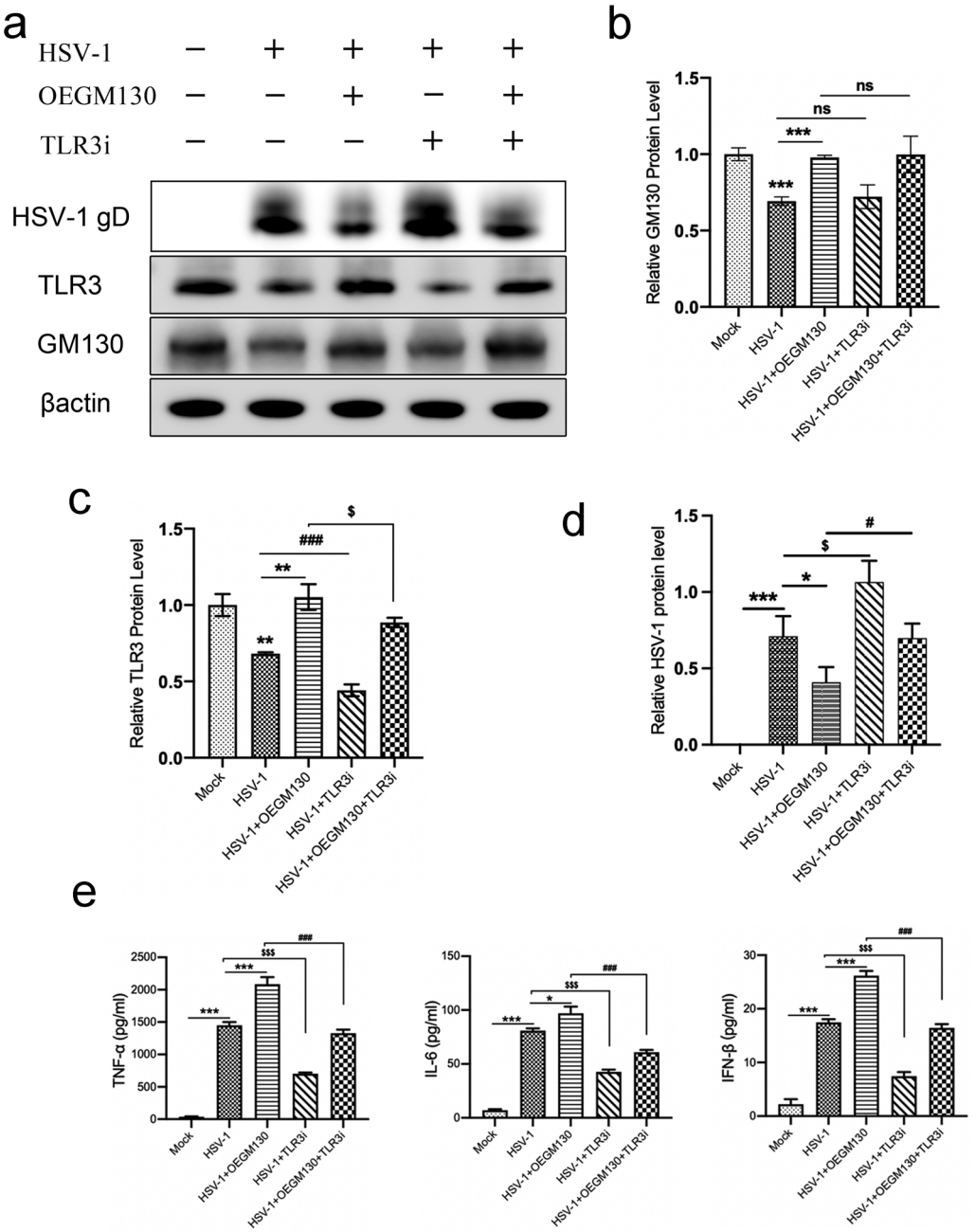

Fig. 8 Effects of TLR3i treatment of GM130 overexpressed BV2 cells on TLR3 and inflammatory cytokines. **a** Protein levels of GM130, TLR3, and HSV-1 after TLR3i treatment were adjusted with βactin as internal reference. The expression levels of the detected proteins in each group were compared with those of the non-infected group. **b** Semi-quantitative results of GM130. **c** Semi-quantitative results of TLR3. **d** Semi-quantitative results of HSV-1 gD. **e** Secretion levels of the inflammatory cytokines IFN-β, TNF-α, and IL-6 after treatment with (TLR3i). Data are obtained through three independent replicates, expressed as X ± SD, and statistically analyzed between the two groups using a t-test. A comparison between the two groups is marked with a dashed line. ns, $p > 0.05$; *, #, $p < 0.05$; **, ##, $p < 0.01$; ***, ###, $p < 0.001$

of GM130 and fragmentation of the GA structure. The mechanism for the decrease in GM130 is associated with the activation of cleaved-caspase 3, a key enzyme in apoptosis, which shears and degrades GM130 [32]. In our study, the level of GM130 decreased in BV2 cells infected with HSV-1, while the structures of GA were fragmented and dispersed in the cytoplasm of BV2 cells infected with HSV-1; these changes of GA mentioned above were also observed in BV2 cells with GM130 knockdown. Interestingly, knocking down GM130 led

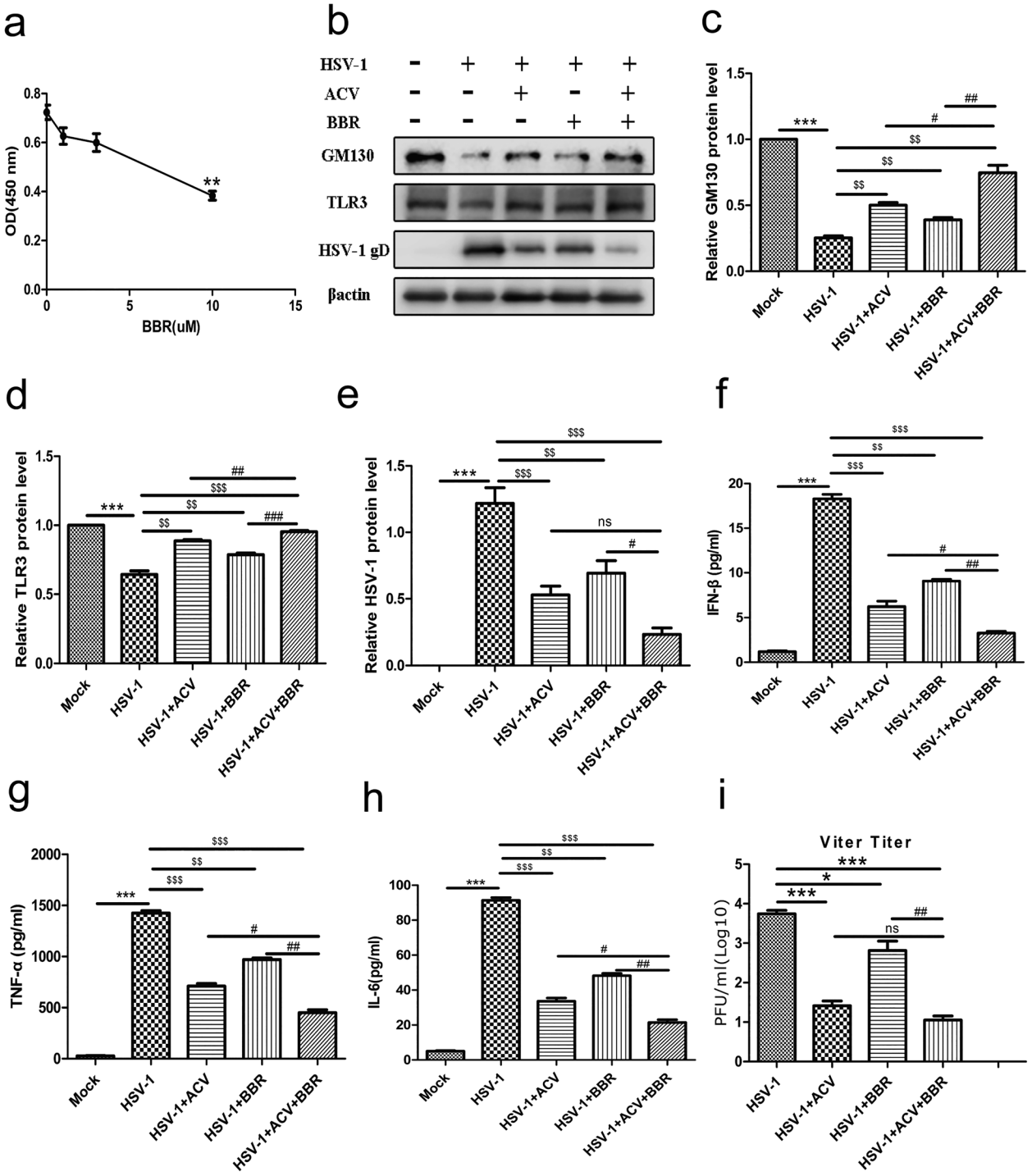

Fig. 9 Effect of berberine (BBR) combined with acyclovir (ACV) on GM130 on TLR3 and inflammatory cytokines. **a** Cellular activity of cells treated with different concentrations of BBR for 24 h. Selection of BBR at a concentration of 3 μM pretreated for 12 h followed by HSV-1 infection for 12 h, and collection of samples. Cells are pretreated with ACV (3 μM) for 12 h and infected with HSV-1 for 12 h. **b** Protein levels of GM130, TLR3, and HSV-1 treated with BBR and ACV were adjusted with βactin as the internal reference. The expression levels of the detected proteins in each group were compared with those of the uninfected group. **c** Semi-quantitative results of GM130. **d** Semi-quantitative results of TLR3. **e** Semi-quantitative results of HSV-1-gD. **f**–**h** Secretion levels of the inflammatory cytokines IFN-β, TNF-α, and IL-6 after treatment with BBR and ACV. **i** Viral titers are treated with BBR and ACV. Data are obtained through three independent replicates, expressed as X ± SD, and statistically analyzed between the two groups using a t-test. A comparison between the two groups is marked with a dashed line. ns, $p > 0.05$; *, #, $p < 0.05$; **, ##, $p < 0.01$; ***, ###, $p < 0.001$

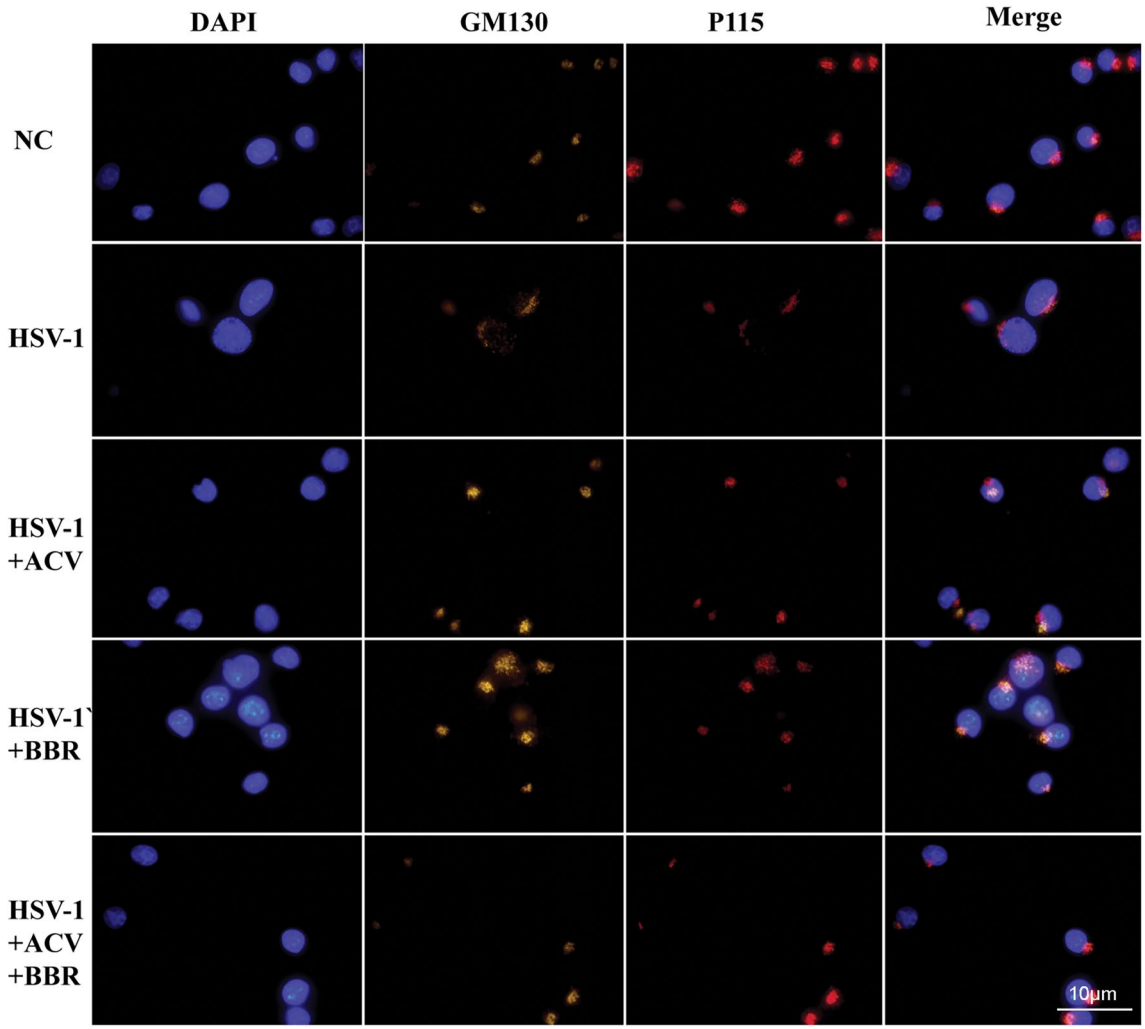

Fig. 10 Structural changes of the Golgi apparatus (GA) in microglia after treatment with acyclovir (ACV) and berberine (BBR). ACV and BBR were pretreated for 12 h before infection, HSV-1 infected cells with MOI = 1, and GA structure (GM130 marker, P115 marker) is observed 12 h after infection. Scale, 10 μm. After ACV treatment, the fluorescently labeled GA structure of GM130 and P115 partially recovered compact perinuclear distribution. After BBR treatment, the fluorescently labeled GA structure of GM130 and P115 partially recovered compact perinuclear distribution. After ACV is combined with BBR, the fluorescently labeled GA structure of GM130 and P115 is further restored to a compact perinuclear distribution. The representative images are obtained from three independent repeated experiments. Scale, 10 μm

to downregulation of TLR3 in uninfected BV2 cells, while in BV2 cells infected with HSV-1, knockdown of GM130 aggravated the damage caused by GA and further downregulated TLR3, with an increased titer of HSV-1; however, the overexpression of GM130 partially restored the structure of GA damaged by HSV-1, and the result was a reversal of decreased TLR3 and increased virus titer. These results suggest that GM130-mediated GA stress can downregulate the level of TLR3 in microglia in response to HSV-1, weakening the immune response of microglia to HSV-1 and resulting in massive replication of HSV-1.

Inhibition of the TLR3 signaling pathway induced by GA stress leads to immune escape from HSV-1. HSV-1 has an immune escape mechanism that targets the innate immune signaling pathway, which is conducive to the spread of the virus and latent infection. Previous studies have found that HSV-1 escapes the immune system through its proteins (e.g., US3, ICP0, and ICP4), which can block multiple links of the TLR3 signaling pathway and lead to reduced secretion of type I interferon and other antiviral inflammatory factors [36]. Therefore, the downregulation of GM130 can reduce the secretion of antiviral inflammatory factors by inhibiting the level of

TLR3 in HSV-1-infected microglia, which may represent a new mode of HSV-1 immune escape.

Furthermore, we found that GM130 affected the release of inflammatory cytokines by regulating the levels of TLR3, which interfered with the replication and proliferation of HSV-1. Our results showed that knockdown of GM130 after infection with HSV-1 inhibited the secretion of IFN-β, TNF-α, and IL-6, but the treatment of the TLR3 agonist could partially inverse the decline of IFN-β, TNF-α, and IL-6. Meanwhile, overexpression of GM130 after HSV-1 infection significantly promoted the secretion of IFN-β, TNF-α, and IL-6, while the TLR3 inhibitor inverses the increase of IFN-β, TNF-α, and IL-6. These results suggested that HSV-1 induces the degradation of GM130 in microglia; however, degradation of GM130 leads to reduced TLR3, along with the decreased release of immunocytokine IFN-β, TNF-α, and IL-6, thus beneficial for the proliferation of HSV-1. The upregulation of GM130 and the protection of GA can elevate the levels of TLR3 and its downstream immune cytokines, reducing the immune escape of HSV-1 and limiting the replication of HSV-1.

Although ACV is the most important drug for HSE treatment, with the increase in the number of drug-resistant viral strains and the growing importance of immunomodulatory therapies, combination therapies may become the main option for HSE treatment in the future. The blood–brain barrier (BBB) is highly permeable to BBR, which is an anti-inflammatory, antiviral, neuroprotective, and immunomodulatory [39]. The immunomodulatory function of BBR has gradually gained attention in recent years [27, 28], and BBR is beneficial for the treatment of animal models of various autoimmune diseases, such as multiple sclerosis [27]. BBR alleviates destructive autoimmune inflammation by inhibiting inflammatory signaling pathways in Th1/Th17 cells, macrophages, and dendritic cells [28, 39]. Our research found that BBR protected GA from fragmentation induced by HSV-1 and reversed the decrease in GM130 levels, suggesting that BBR plays a protective role in GA during HSV-1 infection. Further results suggested that BBR also reverses the reduction of TLR3 and IFN-β, TNF-α, and IL-6 mediated by the decrease in GM130, thus decreasing the titer of HSV-1; these suggested that BBR negatively affects HSV-1 mediated immune escape by promoting TLR3 mediated innate immune response. Interestingly, we found that BBR combined with ACV was more effective than either drug alone. Compared to BBR or ACV alone, the structure of GA was further protected, and TLR3-mediated innate immunity was further enhanced by the combination of BBR and ACV. Therefore, our study suggests that BBR improves the innate immune response and inhibits the titer of HSV-1 and that ACV combined with BBR is more effective in inhibiting HSV-1 than ACV alone. In the future, BBR may be an effective and promising therapeutic agent for HSE due to its low toxicity and cost [40].

In summary, we found that HSV-1 triggered GA stress in microglia, which manifested itself primarily as decreased levels of GM130 and the destruction of GA. Downregulation of GM130 promotes HSV-1 replication by inhibiting TLR3 signaling. These results revealed the possible role of GA as a site of innate immune signal transduction to regulate the TLR3 signaling pathway, which may provide a new signal for the development of immunoregulatory therapies for HSE. Interestingly, we found that BBR protects against GA and upregulates the TLR3 signaling pathway to enhance the anti-HSV-1 immune response and that the combination of BBR and ACV shows promise as a new strategy for HSE. A limitation of this study is that it did not explore the specific mechanism of GM130 reduction in response to HSV-1 infection in microglia, which will be explored further in our subsequent experiments.

Conclusion

GM130 affects secretion levels of IFN-β, TNF-α, and IL-6 by regulating the level of TLR3, inhibiting virus replication, and playing an antiviral immune response. This suggests that GA may be an important site for the regulation of the TLR3 signaling pathway. BBR can protect against GA and upregulate the TLR3 signaling pathway to promote an antiviral immune response. The combination of BBR and ACV is expected to be a novel strategy for the treatment of HSE.

Supplementary Information

The online version contains supplementary material available at https://doi.org/10.1186/s12985-024-02492-x.

Additional file 1.

Additional file 2.

Additional file 3.

Acknowledgements

Not applicable.

Author contributions

XQC searched and reviewed the literature, drafted the manuscript and revised the manuscript; JL, JXL and HNZ discussed and revised the manuscript; WL designed and formulated the review theme and revised and finalized the manuscript. All authors read and approved the final manuscript.

Funding

This work was funded by the Natural Science Foundation of Hunan Province (#2024JJ5477).

Availability of data and materials
No datasets were generated or analysed during the current study.

Declarations

Ethics approval and consent to participate
Not applicable.

Consent for publication
Not applicable.

Competing interests
The authors declare no competing interests.

Received: 24 February 2024 Accepted: 6 September 2024
Published online: 16 September 2024

References

1. Silva MT. Viral encephalitis. Arq Neuropsiquiatr. 2013;71(9b):703–9. https://doi.org/10.1590/0004-282x20130155.
2. Granerod J, Tam CC, Crowcroft NS, Davies NW, Borchert M, Thomas SL. Challenge of the unknown: a systematic review of acute encephalitis in non-outbreak situations. Neurology. 2010;75(10):924–32. https://doi.org/10.1212/WNL.0b013e3181f11d65.
3. Gnann JW Jr, Whitley RJ. Herpes simplex encephalitis: an update. Curr Infect Dis Rep. 2017;19(3):13. https://doi.org/10.1007/s11908-017-0568-7.
4. Armangue T, Spatola M, Vlagea A, Mattozzi S, Cárceles-Cordon M, Martinez-Heras E, et al. Frequency, symptoms, risk factors, and outcomes of autoimmune encephalitis after herpes simplex encephalitis: a prospective observational study and retrospective analysis. Lancet Neurol. 2018;17(9):760–72. https://doi.org/10.1016/s1474-4422(18)30244-8.
5. Lundberg P, Ramakrishna C, Brown J, Tyszka JM, Hamamura M, Hinton DR, et al. The immune response to herpes simplex virus type 1 infection in susceptible mice is a major cause of central nervous system pathology resulting in fatal encephalitis. J Virol. 2008;82(14):7078–88. https://doi.org/10.1128/jvi.00619-08.
6. Verzosa AL, McGeever LA, Bhark SJ, Delgado T, Salazar N, Sanchez EL. Herpes simplex virus 1 infection of neuronal and non-neuronal cells elicits specific innate immune responses and immune evasion mechanisms. Front Immunol. 2021;12:644664. https://doi.org/10.3389/fimmu.2021.644664.
7. Kawai T, Akira S. The role of pattern-recognition receptors in innate immunity: update on Toll-like receptors. Nat Immunol. 2010;11(5):373–84. https://doi.org/10.1038/ni.1863.
8. Sheridan GK, Murphy KJ. Neuron-glia crosstalk in health and disease: fractalkine and CX3CR1 take centre stage. Open Biol. 2013;3(12): 130181. https://doi.org/10.1098/rsob.130181.
9. Katzilieris-Petras G, Lai X, Rashidi AS, Verjans G, Reinert LS, Paludan SR. Microglia activate early antiviral responses upon herpes simplex virus 1 entry into the brain to counteract development of encephalitis-like disease in mice. J Virol. 2022;96(6):e0131121. https://doi.org/10.1128/jvi.01311-21.
10. Alexopoulou L, Holt AC, Medzhitov R, Flavell RA. Recognition of double-stranded RNA and activation of NF-kappaB by Toll-like receptor 3. Nature. 2001;413(6857):732–8. https://doi.org/10.1038/35099560.
11. Stetson DB, Medzhitov R. Type I interferons in host defense. Immunity. 2006;25(3):373–81. https://doi.org/10.1016/j.immuni.2006.08.007.
12. Takeda K, Akira S. Toll-like receptors in innate immunity. Int Immunol. 2005;17(1):1–14. https://doi.org/10.1093/intimm/dxh186.
13. Lafaille FG, Ciancanelli MJ, Studer L, Smith G, Notarangelo L, Casanova JL, et al. Deciphering human cell-autonomous anti-HSV-1 immunity in the central nervous system. Front Immunol. 2015;6:208. https://doi.org/10.3389/fimmu.2015.00208.
14. Liu Z, Guan Y, Sun X, Shi L, Liang R, Lv X, et al. HSV-1 activates NF-kappaB in mouse astrocytes and increases TNF-alpha and IL-6 expression via Toll-like receptor 3. Neurol Res. 2013;35(7):755–62. https://doi.org/10.1179/016164113x13703372991516.
15. Minagawa H, Hashimoto K, Yanagi Y. Absence of tumour necrosis factor facilitates primary and recurrent herpes simplex virus-1 infections. J Gen Virol. 2004;85(Pt 2):343–7. https://doi.org/10.1099/vir.0.19627-0.
16. Gao D, Ciancanelli MJ, Zhang P, Harschnitz O, Bondet V, Hasek M, et al. TLR3 controls constitutive IFN-β antiviral immunity in human fibroblasts and cortical neurons. J Clin Investig. 2021. https://doi.org/10.1172/jci134529.
17. Sancho-Shimizu V, Zhang SY, Abel L, Tardieu M, Rozenberg F, Jouanguy E, et al. Genetic susceptibility to herpes simplex virus 1 encephalitis in mice and humans. Curr Opin Allergy Clin Immunol. 2007;7(6):495–505. https://doi.org/10.1097/ACI.0b013e3282f151d2.
18. Zhang SY, Herman M, Ciancanelli MJ, Pérez de Diego R, Sancho-Shimizu V, Abel L, et al. TLR3 immunity to infection in mice and humans. Curr Opin Immunol. 2013;25(1):19–33. https://doi.org/10.1016/j.coi.2012.11.001.
19. Tao Y, Yang Y, Zhou R, Gong T. Golgi Apparatus: An Emerging Platform for Innate Immunity. Trends Cell Biol. 2020;30(6):467–77. https://doi.org/10.1016/j.tcb.2020.02.008.
20. Nakamura N. Emerging new roles of GM130, a cis-Golgi matrix protein, in higher order cell functions. J Pharmacol Sci. 2010;112(3):255–64. https://doi.org/10.1254/jphs.09r03cr.
21. Figueroa-Lozano S, Valk-Weeber RL, van Leeuwen SS, Dijkhuizen L, de Vos P. Dietary N-Glycans from bovine lactoferrin and TLR modulation. Mol Nutr Food Res. 2018. https://doi.org/10.1002/mnfr.201700389.
22. Sun J, Duffy KE, Ranjith-Kumar CT, Xiong J, Lamb RJ, Santos J, et al. Structural and functional analyses of the human Toll-like receptor 3: role of glycosylation. J Biol Chem. 2006;281(16):11144–51. https://doi.org/10.1074/jbc.M510442200.
23. Song D, Hao J, Fan D. Biological properties and clinical applications of berberine. Front Med. 2020;14(5):564–82. https://doi.org/10.1007/s11684-019-0724-6.
24. Yarla NS, Bishayee A, Sethi G, Reddanna P, Kalle AM, Dhananjaya BL, et al. Targeting arachidonic acid pathway by natural products for cancer prevention and therapy. Semin Cancer Biol. 2016;40–41:48–81. https://doi.org/10.1016/j.semcancer.2016.02.001.
25. Hesari A, Ghasemi F, Cicero AFG, Mohajeri M, Rezaei O, Hayat SMG, et al. Berberine: a potential adjunct for the treatment of gastrointestinal cancers? J Cell Biochem. 2018;119(12):9655–63. https://doi.org/10.1002/jcb.27392.
26. Pirillo A, Catapano AL. Berberine, a plant alkaloid with lipid- and glucose-lowering properties: From in vitro evidence to clinical studies. Atherosclerosis. 2015;243(2):449–61. https://doi.org/10.1016/j.atherosclerosis.2015.09.032.
27. Ehteshamfar SM, Akhbari M, Afshari JT, Seyedi M, Nikfar B, Shapouri-Moghaddam A, et al. Anti-inflammatory and immune-modulatory impacts of berberine on activation of autoreactive T cells in autoimmune inflammation. J Cell Mol Med. 2020;24(23):13573–88. https://doi.org/10.1111/jcmm.16049.
28. Haftcheshmeh SM, Abedi M, Mashayekhi K, Mousavi MJ, Navashenaq JG, Mohammadi A, et al. Berberine as a natural modulator of inflammatory signaling pathways in the immune system: focus on NF-κB, JAK/STAT, and MAPK signaling pathways. Phytotherapy Res PTR. 2022;36(3):1216–30. https://doi.org/10.1002/ptr.7407.
29. Wang ZZ, Li K, Maskey AR, Huang W, Toutov AA, Yang N, et al. A small molecule compound berberine as an orally active therapeutic candidate against COVID-19 and SARS: a computational and mechanistic study. FASEB J Off Publ Feder Am Soc Exp Biol. 2021;35(4):e21360. https://doi.org/10.1096/fj.202001792R.
30. Manglani M, Poley M, Kumar A, McSherry G, Ericson JE. Anti-NMDAR encephalitis after neonatal HSV-1 infection in a child with low TLR-3 function. Pediatrics. 2021. https://doi.org/10.1542/peds.2020-035824.
31. Mielcarska MB, Skowrońska K, Wyżewski Z, Toka FN. Disrupting neurons and glial cells oneness in the brain-the possible causal role of herpes simplex virus type 1 (HSV-1) in Alzheimer's disease. Int J Mol Sci. 2021. https://doi.org/10.3390/ijms23010242.
32. He Q, Liu H, Huang C, Wang R, Luo M, Lu W. Herpes simplex virus 1-induced blood-brain barrier damage involves apoptosis associated with gm130-mediated golgi stress. Front Mol Neurosci. 2020;13:2. https://doi.org/10.3389/fnmol.2020.00002.

33. Colonna M, Butovsky O. Microglia function in the central nervous system during health and neurodegeneration. Annu Rev Immunol. 2017;35:441–68. https://doi.org/10.1146/annurev-immunol-051116-052358.
34. Uyar O, Laflamme N, Piret J, Venable MC, Carbonneau J, Zarrouk K, et al. An early microglial response is needed to efficiently control herpes simplex virus encephalitis. J Virol. 2020. https://doi.org/10.1128/jvi.01428-20.
35. Reinert LS, Lopušná K, Winther H, Sun C, Thomsen MK, Nandakumar R, et al. Sensing of HSV-1 by the cGAS-STING pathway in microglia orchestrates antiviral defence in the CNS. Nat Commun. 2016;7:13348. https://doi.org/10.1038/ncomms13348.
36. Zhu H, Zheng C. The race between host antiviral innate immunity and the immune evasion strategies of herpes simplex virus 1. Microbiol Mol Biol Rev MMBR. 2020. https://doi.org/10.1128/mmbr.00099-20.
37. Li T, You H, Mo X, He W, Tang X, Jiang Z, et al. GOLPH3 Mediated Golgi Stress Response in modulating N2A cell death upon oxygen-glucose deprivation and reoxygenation injury. Mol Neurobiol. 2016;53(2):1377–85. https://doi.org/10.1007/s12035-014-9083-0.
38. Ignashkova TI, Gendarme M, Peschk K, Eggenweiler HM, Lindemann RK, Reiling JH. Cell survival and protein secretion associated with Golgi integrity in response to Golgi stress-inducing agents. Traffic. 2017;18(8):530–44. https://doi.org/10.1111/tra.12493.
39. Habtemariam S. Berberine pharmacology and the gut microbiota: a hidden therapeutic link. Pharmacol Res. 2020;155:104722. https://doi.org/10.1016/j.phrs.2020.104722.
40. Derosa G, Maffioli P. Alkaloids in the nature: pharmacological applications in clinical practice of berberine and mate tea. Curr Top Med Chem. 2014;14(2):200–6. https://doi.org/10.2174/1568026613666131213155252.

Publisher's Note